

ARTICLE

<https://doi.org/10.1038/s42004-019-0218-0>

OPEN

Reproduction of vesicles coupled with a vesicle surface-confined enzymatic polymerisation

Minoru Kurisu ¹, Harutaka Aoki¹, Takehiro Jimbo¹, Yuka Sakuma¹, Masayuki Imai ^{1*},
Sandra Serrano-Luginbühl² & Peter Walde ²

Molecular assembly systems that have autonomous reproduction and Darwinian evolution abilities can be considered as minimal cell-like systems. Here we demonstrate the reproduction of cell-sized vesicles composed of AOT, i.e., sodium bis-(2-ethylhexyl) sulfosuccinate, coupled with an enzymatic polymerisation reaction occurring on the surface of the vesicles. The particular reaction used is the horseradish peroxidase-catalysed polymerisation of aniline with hydrogen peroxide as oxidant, which yields polyaniline in its emeraldine salt form (PANI-ES). If AOT micelles are added during this polymerisation reaction, the AOT - PANI-ES vesicles interact with the AOT molecules in the external solution and selectively incorporate them in their membrane, which leads to a growth of the vesicles. If the AOT vesicles also contain cholesterol, the vesicles not only show growth, but also reproduction. An important characteristic of this reproduction system is that the AOT-based vesicles encourage the synthesis of PANI-ES and PANI-ES promotes the growth of AOT vesicles.

¹Department of Physics, Graduate School of Science, Tohoku University, 6-3 Aoba, Aramaki, Aoba, Sendai 980-8578, Japan. ²Department of Materials, ETH Zürich, Vladimir-Prelog-Weg 5, CH-8093 Zürich, Switzerland. *email: imai@bio.phys.tohoku.ac.jp

One way to try to understand “What is Life?” is to attempt the synthesis of minimal cells which contain the essence of “life”¹. Here, we consider “minimal cells” as molecular assembly systems that show autonomous reproduction and Darwinian evolution features. Thus, a minimal cell is characterised by three important properties; (i) metabolism that extracts usable energy and chemical resources from the environment, (ii) self-reproduction that is recursive growth and division of a compartment, and (iii) evolvability that requires the essential biological aspects of genetic variation and its phenotypic expression^{2–4}.

Among several gateways towards the synthesis of minimal cells, one of the soft matter approaches focuses on constructing minimal cells using well-defined vesicle membrane-forming molecules to hopefully reveal some of the underlying physical chemical mechanisms of the growth and reproduction of living systems^{5–8}. In this approach, preformed vesicles take up precursors of the membrane molecules from the environment, which are then transformed by a chemical modification into the membrane molecules of pre-existing vesicles. The transformed membrane molecules incorporate into the vesicle membrane, which leads to vesicle growth or even division into independent vesicles having similar properties as the mother vesicles^{9–12}. Such simple reproducing vesicle systems were initially developed by Luisi’s group^{10,11}, whereby the growth and division of oleic acid vesicles was induced by the hydrolysis of oleic anhydride into oleic acid and oleate. The group of Szostak developed a cyclic reproduction of *multilamellar* fatty acid vesicles^{13,14}. By addition of oleate micelles, spherical multilamellar oleic acid vesicles divided into multilamellar daughter vesicles through a growth to thread-like vesicles. Upon further micelle addition, the growth-division cycle continued in a cyclic manner. A unique feature of this mechanism is that growth followed by division is promoted by an affinity between specific chemicals (e.g. dipeptide) and fatty acids, which might bring Darwinian evolution¹⁵. A chemically completely different reproducing giant vesicle system was studied by Sugawara’s group^{16,17}. It is based on the design of engineered amphiphiles and their precursor molecules. The precursors are transformed to the amphiphiles by hydrolysis, which results in the growth and division of vesicles composed of the amphiphiles. In addition, the same group succeeded to couple this vesicle reproduction system with the amplification of encapsulated DNAs¹⁸. A similar protocol was developed by Devaraj’s group^{19,20}.

In this study we demonstrate a specific example of the reproduction of giant unilamellar vesicles (GUVs) coupled with a vesicle surface-confined enzymatic polymerisation reaction. When aniline is polymerised with horseradish peroxidase (HRP) and hydrogen peroxide (H₂O₂) in the presence of sodium bis-(2-ethylhexyl) sulfosuccinate (AOT) vesicles, oligomeric and polymeric products are obtained which have characteristic properties of the emeraldine salt form of linear *para*-NC coupled polyaniline, abbreviated as PANI-ES²¹. Whenever the term “PANI-ES” is used we mean polyaniline products which consist of PANI-ES units. In this system, determining the molar mass of the formed products is not possible, since the final polymers become insoluble after AOT removal^{22,23}. The reaction occurs localised on the surface of the vesicles (Supplementary Fig. 1 and Supplementary Note 1)^{21–23} through (PANI-ES) N-H...O-S (AOT) hydrogen bonding²⁴, steric or electrostatic interactions²⁵ (Supplementary Fig. 2 and Supplementary Note 2). In this reaction, the vesicles serve as a kind of “template”, which means that the outcome of this vesicle surface-confined reaction is influenced in a positive way by the vesicles²⁶.

In the work presented now, we find that the enzymatically formed PANI-ES on the AOT vesicles interact (through a kind of

molecular recognition) with AOT molecules which are added to the external solution so that they are selectively incorporated into the AOT vesicle membrane. This results in the growth of the vesicles. The important observation is that the AOT vesicles not only promote the enzymatic synthesis of PANI-ES through the vesicle template effect, but that the obtained PANI-ES is also a kind of “information molecule” which promotes vesicle growth. This mutual promotion system fulfills the physical requirements of minimal cells^{27,28}. In addition, by introducing to the AOT vesicle/PANI-ES system a second amphiphile having a negative molecular spontaneous curvature^{5–7}, we succeed in realising not only the growth of vesicles, but also the division of the grown vesicles (reproduction). On the basis of the observed mutual promotion mechanism, we develop a kinetic model, which predicts that this system has the potential for the experimental realisation of recursive reproduction and Darwinian evolution. Thus, the purpose of this study is to show that the “template”-assisted enzymatic polymerisation occurring on the surface of the vesicles, known as PANI-ES synthesis on AOT vesicles, brings the reproduction of vesicles by feeding membrane molecules, which is a promising system for the development of minimal cells.

Results

Enzymatic polymerisation of aniline on AOT vesicles. An important feature of the enzymatic polymerisation of aniline in the presence of AOT vesicles^{21,22} is the interaction between the vesicle-forming amphiphile and the formed products through specific PANI-ES-amphiphile contacts (Supplementary Fig. 2 and Supplementary Note 2). In agreement with previous studies using large unilamellar vesicle (LUV) suspensions²³, we demonstrate that the outcome of this vesicle-assisted enzymatic polymerisation of aniline depends on the chemical structure of the vesicle template-forming molecules. Depending on vesicle type and experimental conditions, the obtained polyaniline products differ in their UV/vis/NIR absorption spectrum (Fig. 1). An important point is the fact that the reaction is localised on the surface of AOT vesicles and that the formed products (rich in PANI-ES structural units) are also localised on the vesicle surface²¹. For this to occur there must be attractive interactions between the vesicle surface and the polymerisation products (Supplementary Fig. 2 and Supplementary Note 2)^{24,25}.

To first re-examine and also extend earlier investigations on the effect of the polar head group structure of vesicle-forming amphiphiles on the PANI product formation²³, we prepared three types of LUVs. They were composed of either (i) a zwitterionic phospholipid (DOPC), (ii) anionic phospholipids (DOPA, DOPG, or DOPS) or (iii) anionic amphiphiles with a sulfate or sulfonate head group (porcine brain sulfatides, which is a mixture of glycosphingolipid sulfates, AOT, or SDBS in a 1:1 (mol/mol) mixture with decanoic acid, abbreviated as SDBS/DA). DOPC stands for 1,2-dioleoyl-*sn*-glycero-3-phosphocholine, DOPA for 1,2-dioleoyl-*sn*-glycero-3-phosphate sodium salt, DOPG for 1,2-dioleoyl-*sn*-glycero-3-phospho-(1'-*rac*-glycerol) sodium salt, DOPS for 1,2-dioleoyl-*sn*-glycero-3-phospho-L-serine, and SDBS for sodium dodecylbenzenesulfonate. Since pure SDBS in dilute aqueous solution does not form vesicles²⁹, LUVs composed of SDBS and DA were prepared³⁰. The polymerisation reaction was triggered by adding H₂O₂ (oxidant) to the LUV suspensions (20 mM NaH₂PO₄ solution, pH = 4.3) containing aniline and HRP. HRP is the catalyst for initiating the reaction after being oxidised by H₂O₂²¹. Under the optimal conditions elaborated for AOT LUVs, see Materials and Methods, the oxidation of aniline occurs very rapidly²¹ within less than one minute, 95% of the added H₂O₂ is reduced and 75% of the aniline is oxidised (Fig. 3 of ref. 21). For all vesicle systems which we tested as potential

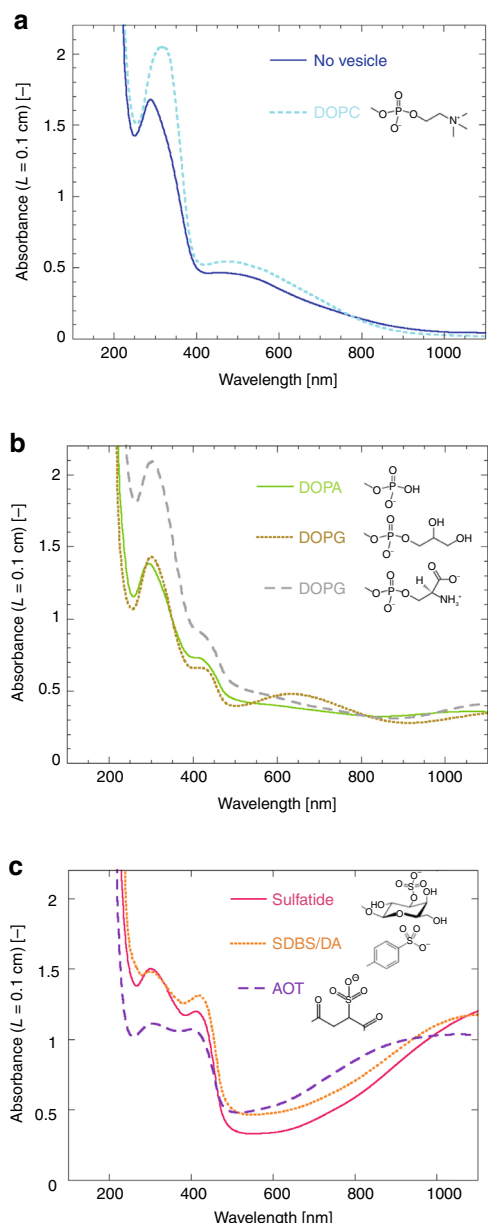


Fig. 1 UV/vis/NIR absorption spectra of the polymerisation products. The products were obtained upon oxidation and polymerisation of aniline (4.0 mM) at pH = 4.3 (20 mM NaH_2PO_4) with HRP (0.92 μM) and H_2O_2 (4.5 mM) for 24 h at 25 °C in the presence of LUVs formed from either **a** DOPC; **b** DOPA, DOPG, or DOPS; **c** bovine brain sulfatides, SDBS/DA (1:1), or AOT. For all these measurements, the amphiphile concentration was 3.0 mM. Path length (L): 0.1 cm. The spectrum recorded for a reaction mixture which did not contain vesicles is also shown in (a). The chemical structures of the head group of each amphiphile are given as insets

templates for the reaction, the UV/vis/NIR absorption spectra of the reaction mixtures were measured after running the reaction for 24 h at room temperature (about 25 °C). The recorded spectra clearly depend on the type of LUVs used (Fig. 1). With zwitterionic—and overall neutral—DOPC LUVs (Fig. 1a), the spectrum shows strong absorption in the range of 280–320 nm ($\pi \rightarrow \pi^*$ transition), a broad peak at 500 nm (indicative for extensive branching³¹ and phenazine unit formation²⁵), and very low absorption at around 1000 nm (absence of $\pi \rightarrow$ polaron transition) as well as absence of an absorption peak at about 400 nm (no polaron $\rightarrow \pi^*$ transition³²), i.e., absence of

characteristic transitions for PANI-ES in polaron state with its unpaired electrons^{21,22,33}. Therefore, the UV/vis/NIR absorption measurements indicate that highly branched PANI and/or phenazine units-rich polymers were obtained in the presence of DOPC vesicles. Thus, no significant “template” effect was observed for the polymerisation in the presence of DOPC LUVs. In a control experiment, the enzymatic polymerisation of aniline was also performed without vesicles. The obtained products showed a very similar absorption spectrum to that with the DOPC vesicles (Fig. 1a) with product precipitation upon storage. For the reaction in the presence of anionic phospholipid LUVs (DOPG, DOPA, or DOPS), new weak bands appear at 440 nm and 1000 nm (Fig. 1b, and for data obtained with vesicles from the related POPG²³). Thus, only a small amount of PANI-ES structural units in polaron state is synthesised in the presence of anionic phospholipid vesicles. For LUVs prepared from anionic amphiphiles having a sulfonate or sulfate head group (AOT, SDBS/DA (1:1), or porcine brain sulfatides), the spectra have high absorptions at 440 nm and 1000 nm and low absorption at 500 nm, indicating preferential synthesis of PANI-ES (Fig. 1c).

All in all, the HRP-triggered polymerisation of aniline with H_2O_2 as oxidant in the presence of vesicles produces different mixtures of reaction products, depending on the chemical structure of the vesicle membrane-forming amphiphile’s head group. This is in full agreement with findings from similar experiments carried out with micelles or polyelectrolytes as templates³⁶. Especially, the sulfonate or sulfate head group of the membrane-forming molecule is somewhat “encoded” in the chemical structure of PANI-ES through electrostatic, N-H \cdots O-S hydrogen bonding, and steric interactions (Supplementary Fig. 1)^{21,24,25}.

Growth of vesicles coupled with “template” polymerisation.

The first important result from our study is the demonstration that the growth of AOT vesicles can be coupled with the vesicle-assisted enzymatic polymerisation of aniline. In other words vesicle growth is linked to a “template” polymerisation.

If dissolved in pure water at a concentration which is above the critical micellization concentration ($\text{cmc} \approx 2.6$ mM at room temperature³⁴), AOT molecules assemble into micelles; whereas in 100 mM NaH_2PO_4 solution (pH = 4.3) and above the critical concentration for vesicle formation ($\text{cvc} \approx 0.4$ mM²²) AOT forms bilayered vesicles. As a consequence, when a small amount of AOT micelles (in water) is added to an AOT GUV suspension (in NaH_2PO_4 pH = 4.3 solution), the AOT molecules originally constituting the micelles will either form new vesicles or incorporate into the preformed GUV membranes, in analogy to what has been discussed before for fatty acid vesicles³⁷. We then investigated whether AOT GUV growth is observed and whether the simultaneous enzymatic formation of PANI-ES on the surface of the vesicles has a significant influence on the process due to interactions between AOT and PANI-ES (see above).

AOT GUVs were first prepared in 20 mM NaH_2PO_4 solution (pH = 4.3) containing 4.0 mM aniline and 0.92 μM HRP. Afterwards, a solution of 2.0 M H_2O_2 and 20 mM AOT micelles (prepared in pure water) was then micro-injected to a selected target GUV and its size change was analysed (entry #1 in Table 1). It should be noted that the micro-injection of the reactant solutions does not affect the reaction condition significantly (Supplementary Note 3 and Supplementary Fig. 3). To estimate vesicle growth quantitatively, the distance between the target GUV and the tip of the micropipette was fixed by using a double micro-injection technique (Supplementary Fig. 4 and Supplementary Note 4). When this micellar AOT/ H_2O_2 solution was micro-injected, the target GUV maintained its spherical

Table 1 Growth of AOT GUVs for various conditions, as observed by phase contrast light microscopy

entry	AOT GUV suspension (pH = 4.3, 20 mM NaH ₂ PO ₄)		Micro-injection solution		Polymerisation	GUV growth
	aniline ^a	HRP ^b	H ₂ O ₂ ^c	AOT micelles ^d		
#1	✓	✓	✓	✓	✓	1
#2	–	–	✓	✓	–	0.1
#3	–	✓	✓	✓	–	0
#4	✓	–	✓	✓	–	0
#5	✓	✓	–	✓	–	0

Each condition is designated by the entry number shown in the first column. The 2nd and 3rd columns indicate whether the AOT suspension also contained aniline and/or HRP. The 4th and 5th columns indicate whether the micro-injected solution contained H₂O₂ and/or AOT micelles. The 6th column indicates whether “template” polymerisation occurred or not. The observed growth of the AOT GUVs is indicated qualitatively in the 7th column, normalised to that of entry #1. “1” corresponds to the observed growth with the growth rate of $d(A(t)/A(0))/dt = 0.012 \text{ s}^{-1}$ if polymerisation of aniline into PANI-ES products takes place; “0.1” means growth observed but only at about 10% of the extent for the conditions of entry #1; “0” means no growth observed. See also Figs. 2 and 3a

^a[aniline] = 4.0 mM
^b[HRP] = 0.92 μM
^c[H₂O₂] = 2.0 M
^d[AOT] = 20 mM

shape during the initial 17 s (induction period) and then started to grow with deformation into a prolate shape (Fig. 2a and Supplementary Movie 1). During the growth period from 17 to 45 s, the prolate vesicle elongated with time due to a growth of the membrane area caused by the uptake of AOT molecules from the external solution. As seen in Fig. 2a, the image of the vesicle surface became dark with time, which was due to the formation of polyaniline products. Since the reaction takes place on a growing GUV under micro-injection, it is difficult to analyse the polymer product directly. Instead, the PANI-ES synthesized on AOT GUVs with feeding AOT micelles in bulk solution was characterised using UV/vis/NIR absorption spectroscopy (Supplementary Note 5 and Supplementary Fig. 5). The PANI-ES was identical to that obtained in the previous studies.

The synthesis of PANI-ES on the target AOT GUV in the centre of the image shown in Fig. 2a “encouraged”, i.e., promoted, the growth of the vesicle. Time dependent changes of the vesicle surface area, $A(t)$, were estimated by approximating the vesicle shape with an axisymmetric prolate shape using the Surface Evolver software package^{6,35} (Supplementary Fig. 6). The obtained vesicle area is plotted as a function of time (Fig. 3a, entry #1), whereby the vesicle surface area is normalised by the surface area of the initial spherical vesicle, $A(0)$; the error bars represent standard deviations obtained from three different experiments. In the growth stage (between 17 and 45 s), the vesicle area increased linearly with the growth rate of $d(A(t)/A(0))/dt = 0.012 \text{ s}^{-1}$. The analysis of the vesicle growth kinetics based on the elasticity theory of vesicles (Supplementary Note 6 and Supplementary Fig. 7) is shown in Supplementary Note 7 and Supplementary Fig. 8.

For better understanding the observed vesicle growth, several control experiments were performed.

Importance of simultaneous “template” polymerisation for vesicle growth: AOT micelles were micro-injected to AOT GUVs under conditions where no polymerisation took place (Table 1). When aniline and HRP were not present in the external solution (entry #2), the growth of AOT GUVs induced by the micro-injection of AOT micelles and H₂O₂ was remarkably suppressed (growth rate of 0.0013 s^{-1} in the growth stage between 17 and 100 s) (Figs. 2b and 3a, and Supplementary Movie 2). For these experimental conditions, the observed slight AOT GUV growth indicates that some of the AOT molecules which were supplied through addition of the AOT micelle solution incorporated into the preformed GUV membrane, although the extent of uptake was comparatively low. When the preformed GUV suspension did not contain aniline (entry #3) or HRP (entry #4), micro-injection of AOT micelles and H₂O₂ did not result in a growth of

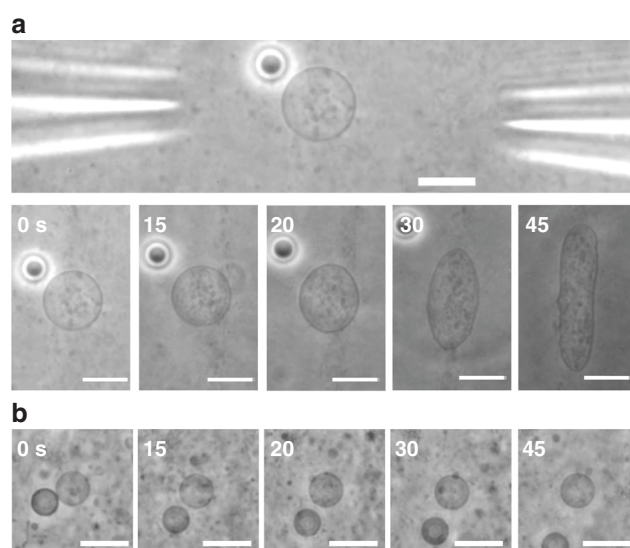


Fig. 2 Phase contrast light microscopy images of AOT GUVs with reactions during the polymerisation reaction. The reaction mixture contained AOT GUVs at pH = 4.3 (20 mM NaH₂PO₄) under various experimental conditions, see Table 1. Length of the scale bars: 20 μm. **a** Entry #1 of Table 1: A 3.0 mM AOT GUV suspension consisting of 4.0 mM aniline and 0.92 μM HRP was first placed into the sample chamber, followed by micro-injection of two different solutions from opposite sites to a selected GUV. With this double micro-injection (Supplementary Fig. 4), the target GUV can be kept in place. The upper image shows the double micro-injection setup with the target GUV in the centre and the two micropipettes on the left and right hand side, respectively. The dark particle with the white halo is an AOT aggregate which was not completely dispersed. From the micropipette on the right hand side, an aqueous solution consisting of AOT micelles (20 mM AOT) and H₂O₂ (2.0 M) was micro-injected. From the micropipette on the left hand side, the pH = 4.3 solution (20 mM NaH₂PO₄) was injected. The lower images show the time dependent changes after starting the micro-injection for $t = 0, 15, 20, 30,$ and 45 s . See also Supplementary Movie 1. **b** Entry #2 of Table 1. Stability of two AOT GUVs in pH = 4.3 solution without aniline and HRP upon micro-injection of AOT micelles (20 mM AOT) and H₂O₂ (2.0 M). The images were taken at $t = 0, 15, 20, 30,$ and 45 s . See also Supplementary Movie 2

the AOT GUV (Fig. 3a). In addition, when only AOT micelles (without H₂O₂) were micro-injected to AOT GUVs in the presence of aniline and HRP (entry #5), there was no AOT GUV growth (Fig. 3a and Supplementary Movie 3). Thus, the synthesis

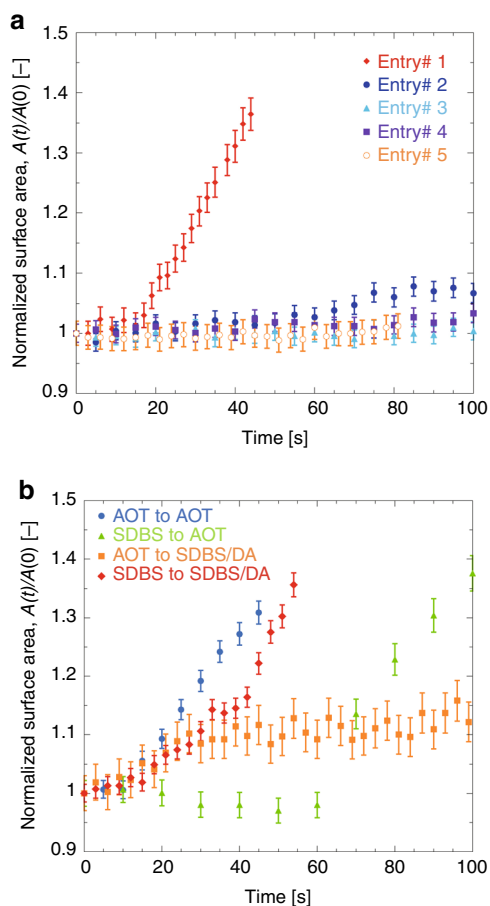


Fig. 3 Growth of AOT or SDBS/DA (1:1) GUVs in response to the micro-injection of AOT or SDBS micelles under various conditions. **a** Experiments with AOT GUVs for the different conditions listed in Table 1. Red diamonds (entry #1): Micro-injection of 2.0 M H_2O_2 and 20 mM AOT micelles dissolved in water to 3.0 mM AOT GUVs prepared in 20 mM NaH_2PO_4 pH = 4.3 solution with 4.0 mM aniline and 0.92 μM HRP. Dark blue closed circles (entry #2): AOT GUV suspension without aniline and without HRP. All other conditions are kept the same as entry #1. Light blue triangles (entry #3): AOT GUV suspension without aniline. All other conditions are kept the same as entry #1. Violet squares (entry #4): AOT GUV suspension without HRP. All other conditions are kept the same as entry #1. Orange open circles (entry #5): The micro-injection solution did not contain H_2O_2 . All other conditions are kept the same as entry #1. **b** Experiments demonstrating the selectivity of the GUV growth, see also Table 2. Blue circles (i): Micro-injection of 2.0 M H_2O_2 and 20 mM AOT SUVs prepared in 20 mM NaH_2PO_4 solution (pH = 4.3) to 3.0 mM AOT GUVs prepared in 20 mM NaH_2PO_4 pH = 4.3 solution with 4.0 mM aniline and 0.92 μM HRP (vesicle growth observed). Green triangles (ii): Micro-injection of 2.0 M H_2O_2 and 100 mM SDBS micelles prepared in 20 mM NaH_2PO_4 solution to AOT GUVs. All other conditions are kept the same as for (i) (vesicle growth observed with delay). Orange squares (iii): Micro-injection of 2.0 M H_2O_2 and 20 mM AOT SUVs prepared in 20 mM NaH_2PO_4 solution (pH = 4.3) to 3.0 mM SDBS/DA (1:1) GUVs prepared in 20 mM NaH_2PO_4 pH = 4.3 solution with 4.0 mM aniline and 0.92 μM HRP (slow vesicle growth observed). Red diamonds (iv): Micro-injection of 2.0 M H_2O_2 and 100 mM SDBS prepared in 20 mM NaH_2PO_4 solution to SDBS/DA (1:1) GUVs. All other conditions are kept the same as for (iii) (vesicle growth observed). The error bars indicate standard deviations estimated from three different experiments

of products consisting of PANI-ES units on the AOT GUV surface remarkably accelerates the growth of AOT GUVs in these AOT micelle feeding experiments. The importance of interactions between PANI-ES and AOT vesicle is also demonstrated by

Table 2 Observed relative growth of four types of GUVs

GUVs with aniline ^a and HRP ^b	Microinjected suspension/solution, containing H_2O_2 ^c			
	SUVs			micelles
	DOPC	DOPA	AOT	SDBS
DOPC GUV	0	0	0	0
DOPA GUV	0	0	0	0
AOT GUV	0	0	1.0	1.1
SDBS/DA GUV	0	0	0.2	0.9

GUVs were prepared from DOPC, DOPA, AOT or SDBS/DA (1:1), all at 3.0 mM total amphiphile concentration in 20 mM NaH_2PO_4 solution, pH = 4.3, upon micro-injection of 20 mM DOPC SUVs, DOPA SUVs, AOT SUVs, or 100 mM SDBS micelles. The observed growth rate of the GUV is normalised by that of the AOT GUV/AOT SUV system [$d(A(t)/A(0))/dt = 0.0086 \text{ s}^{-1}$]. The growth rates were estimated from the growth stages in Fig. 3b; i.e., 10–40 s for AOT to AOT, 60–90 s for SDBS to AOT, 10–100 s for AOT to SDBS/DA, and 10–50 s for SDBS to SDBS/DA
^a[aniline] = 4.0 mM
^b[HRP] = 0.92 μM
^c[H_2O_2] = 2.0 M

additional control experiments (Supplementary Fig. 9, Supplementary Note 8 and Supplementary Movies 4 and 5).

Selectivity of vesicle growth coupled with the synthesis of PANI-ES: The enzymatic polymerisation of aniline in the presence of vesicles produces a mixture of PANI-ES products which consist of aniline repeating units that differ in the way the aniline units are connected (constitutional isomerism) and in their oxidation and protonation state. The PANI product mixture obtained depends on the chemical structure of the vesicle-forming amphiphiles^{23,36}, as is evident from the results shown in Fig. 1. To examine the effect of the type of PANI product mixture obtained on the vesicle growth, four types of GUVs composed of either (i) DOPC, (ii) DOPA, (iii) AOT, or (iv) SDBS/DA (1:1 molar mixture), were prepared in a pH = 4.3 NaH_2PO_4 solution (20 mM) containing aniline and HRP. To each GUV suspension the corresponding amphiphiles were then added by micro-injection together with H_2O_2 : either sonicated DOPC small unilamellar vesicles (DOPC SUVs), DOPA SUVs, AOT SUVs, or SDBS micelles (all prepared in 20 mM NaH_2PO_4 solution, pH = 4.3). The observed growth rates of the GUVs were normalised by that of the growth observed for the AOT GUV/AOT SUV system (Table 2). GUVs from neutral or anionic phospholipids did not show any significant growth. On the other hand, GUVs composed of amphiphiles with a sulfonate head group showed growth (addition of AOT SUVs to AOT GUVs or addition of SDBS micelles to SDBS/DA GUVs). Thus, a coupling between template polymerisation and vesicle growth is observed only for those vesicle systems, which yield products rich in PANI-ES (Fig. 1c) and to which amphiphiles with a sulfonate head group are added. It is worth noting that growth of AOT GUVs was also induced by injection of SDBS micelles (Supplementary Movie 6) and growth of SDBS/DA vesicles was also induced by addition of AOT SUVs (Fig. 3b). Thus, the sulfonate head group is responsible for the observed growth of the vesicles which consist of surface-localised PANI-ES products. This indicates that specific interactions between the polymeric products and the amphiphile head group play an important role in the vesicle growth process. PANI-ES localised on the vesicle surface²¹ interacts with externally added amphiphiles bearing a sulfonate head group which results in a selective incorporation into the vesicle membrane composed of the sulfonate amphiphiles, which leads to a growth of the vesicle. We therefore call the PANI-ES which is produced by the template polymerisation “information polymer”.

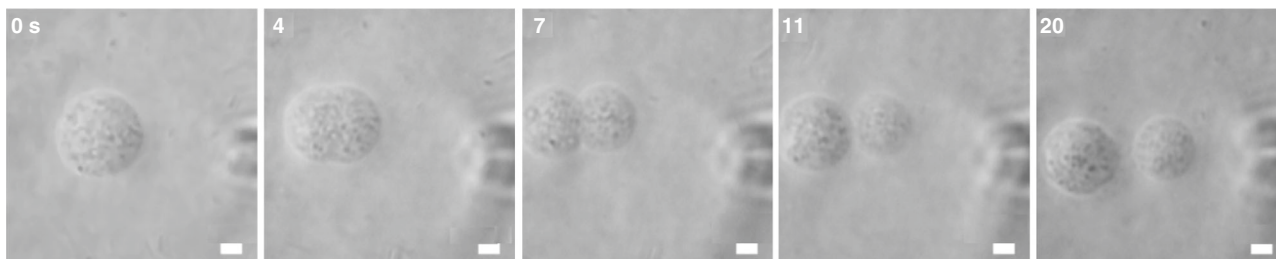


Fig. 4 Phase contrast light microscopy images of a binary AOT/cholesterol GUV, taken during the polymerisation reaction. The binary AOT/cholesterol GUV (9:1, 2.7 mM AOT, 0.3 mM cholesterol), coupled with the synthesis of PANI-ES, showed vesicle growth and division. The binary GUV was prepared in 20 mM NaH_2PO_4 pH = 4.3 solution with 4.0 mM aniline and 0.92 μM HRP, and an aqueous solution of 2.0 M H_2O_2 and 20 mM AOT micelles (prepared in pure water) was micro-injected. The images were taken 0, 4, 7, 11, and 20 s after micro-injection (from left to right). Length of the scale bars: 5 μm . See also Supplementary Movie 7

Putting all experimental data presented in this section together, there is one key observation: AOT (or SDBS/DA) GUVs promote the synthesis of PANI-ES, and PANI-ES promotes the growth of the AOT (or SDBS/DA) GUVs. This *mutual promotion* mechanism is an essential feature of minimal cells^{27,28}, see the kinetic model description in the “Discussion” section.

Reproduction of binary AOT/cholesterol (9:1) GUVs. By feeding spherical AOT GUVs with AOT molecules from the external medium and by coupling this feeding process with a GUV surface-localised enzymatic synthesis of PANI-ES, the AOT GUVs grow to a prolate shape, but they *never* show any vesicle reproduction, i.e., they never show a deformation to the limiting shape consisting of a pair of spheres connected by a narrow neck and a breaking of the neck of the limiting shape. Thus, the shape and topology of the growing vesicles have to be controlled by other means. The deformation and division of vesicles is well described by the elastic theory of membranes^{38,39}. Most importantly, the membrane elasticity model shows that vesicle division is hard to observe in one-component vesicles^{40,41}, which agrees well with experimental observations⁴². Therefore, a second amphiphile having a negative molecular spontaneous curvature (amphiphile with small polar head group and bulky hydrocarbon part) has to be introduced^{5,6}; whereby the coupling between the membrane curvatures and the local amphiphile composition is responsible for the deformation and division of the vesicle^{6,7,43} (Supplementary Note 7 and Supplementary Fig. 8).

Cholesterol with its small polar head group ($-\text{OH}$) and bulky hydrocarbon part, i.e., with its negative spontaneous curvature property, may be suited as the second amphiphile. To test this, we prepared binary GUVs composed of AOT and cholesterol (at a molar ratio of 9:1, 2.7 mM AOT, 0.3 mM cholesterol) in 20 mM NaH_2PO_4 solution (pH = 4.3) containing 4.0 mM aniline and 0.92 μM HRP, and micro-injected to individual binary GUVs a micellar solution consisting of 20 mM AOT and 2.0 M H_2O_2 (prepared in pure water). Immediately after injection, the targeted GUVs started to deform to the limiting shape and then spontaneously divided into two daughter GUVs in about 10 s (Fig. 4 and Supplementary Movies 7 and 8). Although we have no experimental evidence about the compositions of the two daughter vesicles, it is likely that they were the same or very similar. This conclusion is based on a consideration of the characteristic diffusion time, τ , of AOT for a spherical vesicle. It is given by $\tau = R^2/(4D_L)$, where R is the radius of the vesicle and D_L ($=2.7 \times 10^{-11} \text{ m}^2/\text{s}$) is the lateral diffusion coefficient of AOT in the lamellar membrane⁴⁴. For a giant vesicle with $R = 10 \mu\text{m}$ τ is $\sim 0.9 \text{ s}$, which is much smaller than the observed time range for vesicle division ($\sim 10 \text{ s}$). Thus, the two daughter GUVs probably have almost the same AOT/cholesterol membrane composition, although AOT molecules are supplied locally by micro-injection.

The vesicle reproduction was confirmed by carrying out more than 10 identical experiments in which the binary AOT/cholesterol GUVs always showed division, with occasional continuation of the division of the daughter vesicles to a third generation (Supplementary Movie 9). We analysed the vesicle division processes ($n = 4$) induced by the simultaneous micro-injection of AOT micelles and H_2O_2 . When the mother GUV with initial surface area $A(0)$ and volume $V(0)$ showed growth and division, the surface area and volume of the GUV increased to $(1.25 \pm 0.05) \cdot A(0)$ and $(1.05 \pm 0.05) \cdot V(0)$, respectively. The size ratio of daughter to mother vesicles is determined by the balance between the uptake rate of AOT molecules (reduced volume) and the flip-flop rate (normalised preferred area difference) as shown in Supplementary Fig. 7. In addition, the synthesis of PANI-ES was confirmed by recording the UV/vis/NIR absorption spectrum (Supplementary Fig. 10). Thus, we succeeded with the reproduction of AOT-based vesicles due to (i) the presence of a second amphiphile (cholesterol), (ii) a feeding of the vesicles with AOT molecules and (iii) a coupling of the feeding process with the synthesis of an “information polymer” (PANI-ES).

A suggested molecular interpretation which is consistent with the microscopic observations is the following: AOT molecules present in the external solution bind to the formed PANI-ES through electrostatic interactions or hydrogen bonding. This binding decreases the hydrophilicity of the AOT molecules, which promotes incorporation of the bound AOT molecules into the outer monolayer of the AOT/cholesterol GUVs. The incorporated AOT molecules increase the area of the outer monolayer. Flip-flop motions of the AOT molecules coupled with the negative molecular spontaneous curvature of cholesterol relaxes the initially spherical vesicle shape to a prolate shape and then to the limiting shape⁶ (Supplementary Fig. 8). In the limiting shape, cholesterol molecules are excluded from the neck due to the coupling between the molecular shape and the membrane Gaussian curvature, which destabilises the neck and causes vesicle division⁷.

By further injection of AOT micelles and H_2O_2 , the offspring GUVs produced a cascade of multiple small vesicles, i.e., no recursive vesicle reproduction (Supplementary Movie 10). In this type of experiment, H_2O_2 together with *pure AOT micelles* were micro-injected to binary AOT/cholesterol (9:1) GUVs, since it is difficult to incorporate mixed cholesterol-containing AOT micelles. Therefore, the concentration of cholesterol in the binary GUVs decreased with time, which appears to be responsible for the observed division mode transition (a cascade of small vesicles formation). In fact, when AOT micelles and H_2O_2 were micro-injected to binary AOT/cholesterol GUVs consisting of 5 instead of 10 mol% cholesterol, the target GUVs produced a similar cascade of small daughter vesicles from the beginning (Supplementary Movie 11).

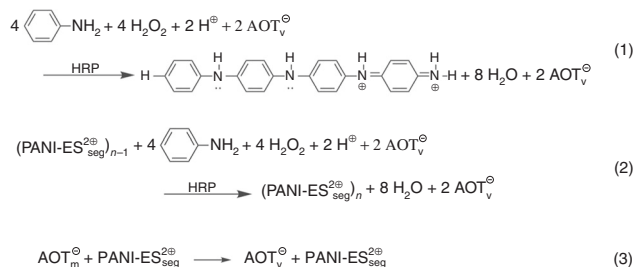


Fig. 5 Stoichiometric equations describing AOT vesicle growth coupled with “template” polymerization. Equation (1): synthesis of the first PANI-ES segment from four aniline molecules on the surface of AOT vesicles in the presence of HRP as catalyst and H_2O_2 as oxidant, where AOT_v^\ominus represents an ionised AOT molecule in the vesicle membrane and the right-hand structure is one half-reduced/half-oxidised and protonated tetraaniline repeating unit (called here “segment”) of PANI-ES ($\text{PANI} - \text{ES}_{\text{seg}}^{2\oplus}$), shown as bipolaron form. Equation (2): chain propagation reaction, where $(\text{PANI} - \text{ES}_{\text{seg}}^{2\oplus})_n$ represents a PANI-ES product consisting of n tetraaniline units (a more detailed reaction scheme for the formation of $\text{PANI} - \text{ES}_{\text{seg}}^{2\oplus}$ is shown in the Supplementary Fig. 12¹). Equation (3): incorporation of AOT molecules from the external micellar AOT solution into the membrane, where AOT_m^\ominus is the ionised AOT molecule supplied by the micelles and $\text{PANI} - \text{ES}_{\text{seg}}^{2\oplus}$ represents a segment of PANI-ES (Supplementary Fig. 2)

Kinetic model of vesicle growth coupled with polymerisation.

In theoretical descriptions of minimal cells, such as the chemoton model⁴⁵, a mutually catalytic reaction network is encapsulated in a compartment (vesicle), whereby for sustaining the compartment-confined reaction network, ingredients and waste have to be transported selectively through the compartment shell (vesicle membrane). To establish such traffic systems, the compartment boundary should be equipped with sophisticated “transport units”, which is an obstacle for the synthesis of minimal cells^{46,47}. In our vesicle model of a simple minimal cell system, the coupling of membrane growth and template polymerisation takes place at the outer surface of the vesicles, which circumvents transmembrane transport and makes the traffic of nutrients and waste easily possible^{48,49}. Our model reaction system, however, does not provide a sustainable vesicle reproduction, as shown in Supplementary Movie 10. In the following, we outline how to develop our existing vesicle reaction system to a sustainable one on the basis of a kinetic model, which we call “template” polymerisation on vesicle (TPV) model (Supplementary Note 9). This TPV model is based on three stoichiometric equations describing three kinetic processes, (i) synthesis of the first PANI-ES segment, (ii) chain propagation, and (iii) incorporation of AOT molecules from the external micellar AOT solution into the membrane, as shown in Fig. 5²¹. The mutual promotion mechanism is captured by this TPV model, independent from the actual length of the formed products consisting of PANI-ES units. The kinetic equations based on this TPV model show synchronised sustainable vesicle growth and “information polymer” production, where the number of polymer segments on the vesicle surface is doubled when the vesicle area doubles (Supplementary Fig. 11a). In this model, the vesicle membrane exhibits exponential growth as shown in Supplementary Fig. 11b. In our vesicle growth experiments, however, the observed membrane growth profile shows linear growth after an induction period (Fig. 3a). This experimentally observed growth profile is explained by the TPV model, when we take into account the experimental constraints, such as polymerisation rate constants, geometry of micro-injection and surface coverage by the polymer product (Supplementary Note 10 and Supplementary Fig. 12). In addition, we experimentally confirmed the

synchronisation between vesicle growth rate and polymer segment production rate, as predicted by the TPV model (Supplementary Note 11 and Supplementary Fig. 13). Another important prediction is that the vesicle growth rate is exponentially accelerated by the polymerisation (Supplementary Fig. 11b inset). This great enhancement indicates advantage of PANI-ES as “information molecule” for promoting vesicle growth.

To achieve reproduction of vesicles, a second amphiphile having a negative spontaneous curvature, such as cholesterol, must participate in the vesicle reproduction process (see the discussion above and Fig. 4). For the binary AOT/cholesterol GUV system, however, cholesterol is not incorporated into the vesicle membrane because cholesterol is not present in the micelles which were added to the GUVs. Moreover, there are no specific interactions between cholesterol and PANI-ES segments. In this case, the concentration of cholesterol in the vesicle membrane monotonically decreases towards zero, i.e., the capability for vesicle division is lost with time (Supplementary Movie 10). The TPV model predicts that a synchronisation between vesicle growth rate and polymer segment production rate would be maintained if the second amphiphile and the information polymer would have mutual catalytic properties like AOT and PANI-ES (Supplementary Fig. 11c). Thus, a key point to attain sustainable vesicle reproduction is to replace cholesterol as second amphiphile by an amphiphile which is directly linked to the enzymatic synthesis of PANI-ES, whereby this second amphiphile must modify the Gaussian curvature modulus through its molecular shape.

We have shown that the enzymatic polymerisation of aniline in the presence of three different types of vesicles composed of either zwitterionic phospholipids (DOPC), anionic phospholipids (DOPA), or synthetic anionic amphiphiles having a sulfonate head group (AOT or SDBS/DA (1:1)), yields products which have different spectroscopic properties, and with this different chemical constitutions and/or oxidation and protonation states, depending on the type of amphiphiles (Fig. 1). Among them, the AOT/PANI-ES pair behaves according to a mutual promotion system, resulting in a sustainable synchronized AOT vesicle growth and the production of PANI-ES. If we regard the PANI-ES/AOT pair as a “species”, and if another polymer/amphiphile pair would also behave in the same way as second “species”, then our TPV model predicts that there will be a competition between two “species”. This would represent a chemical compartment system which is characterised by a natural selection feature, whereby the selection would depend on the rate constants for the species-specific polymerisation and vesicle membrane growth (fitness) (Supplementary Note 12 and Supplementary Fig. 14). Therefore, the “information polymer”/amphiphile system investigated—although being composed of molecules which are not considered prebiotic at all—has the potential for the development of simple chemical systems which have properties that are characteristic of biological systems undergoing Darwinian evolution.

Discussion

We have developed a model for a minimal cell system which consists of the reproduction of vesicles coupled with a “template”-assisted enzymatic polymerisation occurring on the surface of the vesicles. GUVs composed of AOT and cholesterol molecules were first prepared and products consisting of PANI-ES units are obtained from aniline on the vesicle surface, where PANI-ES “interacts with” AOT molecules added to the external solution, and incorporates them into the vesicle membrane, which leads to a growth of the vesicles. Thus, in this model system, PANI-ES plays a role as “information polymer”. An important property of

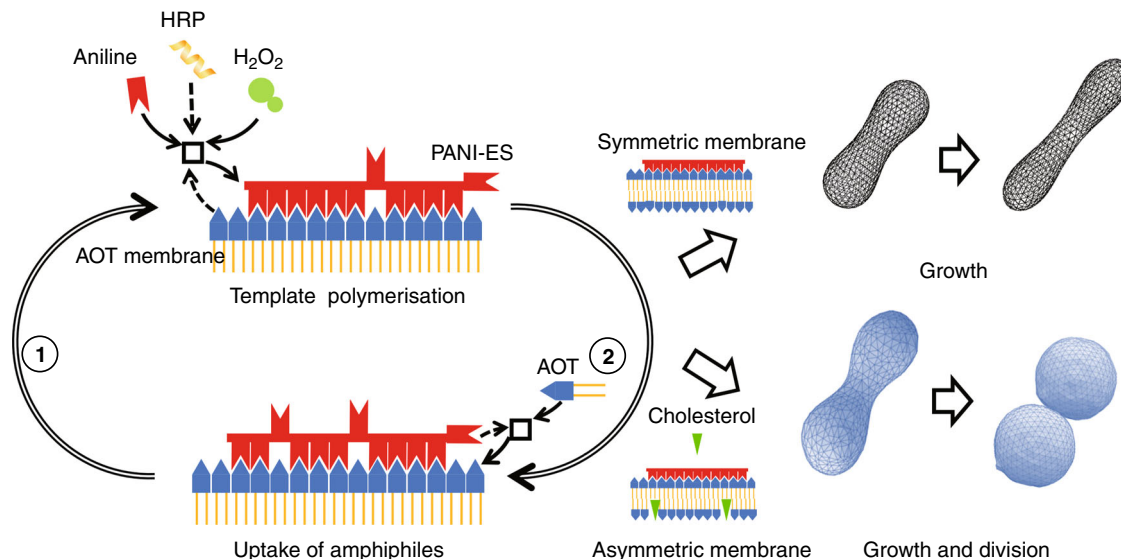


Fig. 6 General scheme of the experimental minimal cell model system presented in this work. This system consists of the “vesicle template”-assisted enzymatic polymerisation of aniline occurring on the surface of AOT vesicles and on the selective uptake of AOT molecules from the external solution by the vesicles through interactions with PANI-ES. In the drawing, solid arrows indicate the participation of reactants and the products of the reaction; dashed arrows indicate the promotion of the reaction (correct coupling of the activated monomers to the growing chain); boxes represent reactions, and double line arrows (1 and 2) indicate the mutual promotion in the system. The mutual promotion results in vesicle growth for vesicles composed of AOT only and vesicle growth and division for binary vesicles composed of AOT and cholesterol. The latter is due to the coupling between the membrane (mean and Gaussian) curvatures and the molecular shapes

the system is that the AOT vesicles promote the synthesis of PANI-ES and that PANI-ES promotes the growth of the AOT vesicles. Conceptually, such mutual promotion property can be seen as an essential feature of minimal cells. In addition to AOT, the second amphiphile, cholesterol, plays an important role. It has a different molecular shape than AOT and induces a negative spontaneous membrane curvature. With this, cholesterol is responsible for vesicle division to occur once the vesicle is grown, through a coupling between vesicle membrane curvatures (mean and Gaussian curvature) and local molecular composition. A general scheme of the system investigated is summarized in Fig. 6. Since PANI-ES is not coupled with the uptake of cholesterol by the vesicle membrane, the vesicle reproduction is limited and will only last for a few generations.

On the basis of our experimental observations we developed a kinetic model of the particular vesicle-assisted polymerisation (called “TPV model”). This TPV model predicts that the reproduction of vesicles becomes recursive when the second amphiphile incorporates into the vesicles through interactions with the formed “information polymer”. In addition, a chemical version of the Darwinian evolution mechanism is expected to emerge when a second “information polymer” formed on the surface of the vesicles constituted by the second amphiphile couples with the growth of the membrane formed by the second amphiphile (emergence of new species). Thus, the reproduction of vesicles coupled with the vesicle-assisted polymerisation system contains (i) a kind of metabolism which extracts usable molecules from the environment, (ii) reproduction, i.e., growth and division of vesicles, and (iii) chemical evolvability, i.e., a “struggle” for the existence of either of two “amphiphile/information polymer” pairs (species). In other words, PANI-ES and AOT vesicles play roles as information tape and general constructor, respectively, if analogy is made to the self-reproducing automaton proposed by von Neumann⁵⁰. Of course this model system is very different from any known biological system and further investigations are necessary. However, our work may be of interest from a conceptual point of view, not only for researchers dealing with

prebiotic compartmentalisation, i.e., protocells, or minimal cells, but also for those investigating fundamental aspects of soft, dynamic compartment systems.

Methods

Amphiphiles used for vesicle and micelle preparation. AOT (sodium bis-(2-ethylhexyl) sulfosuccinate, purity >99%, Catalogue No. 86139) and SDBS (sodium dodecylbenzenesulfonate, hard type, >95%, D0990) were purchased from Sigma-Aldrich Japan (Tokyo, Japan) and Tokyo Chemical Industry (Tokyo, Japan), respectively. DOPC (1,2-dioleoyl-*sn*-glycero-3-phosphocholine, >99%, 850375), DOPA (1,2-dioleoyl-*sn*-glycero-3-phosphate sodium salt, >99%, 840875), DOPG (1,2-dioleoyl-*sn*-glycero-3-phospho-(1'-*rac*-glycerol) sodium salt, >99%, 840475), DOPS (1,2-dioleoyl-*sn*-glycero-3-phospho-L-serine, >99%, 840035), porcine brain sulfatides (as ammonium salt, >99%, 131305) and cholesterol (ovine wool, >98%, 700000) were purchased from Avanti Polar Lipids, Inc. (AL, USA), and DA (decanoic acid, >99%, 041-23256) was from Wako Pure Chemical Industries (Osaka, Japan). The amphiphiles were used without further purification and dissolved in chloroform at 10 mM and stored at -20°C as stock solutions.

Reagents for the polymerisation of aniline. Aniline (>99%), hydrogen peroxide (guaranteed grade, 30% in water, =9.8 M), sodium dihydrogenphosphate (NaH_2PO_4) dihydrate (>99.0%), phosphoric acid (H_3PO_4 , guaranteed grade, 85% in water) and chloroform (>99%) were purchased from Wako Pure Chemical Industries (Osaka, Japan). Horseradish peroxidase isoenzyme C (HRP, Grade I, 285 U/mg, RZ > 3, Lot No. 73120) was from Toyobo Enzymes (Osaka, Japan). The peroxidase concentration was determined spectrophotometrically by using $\epsilon_{403} = 1.02 \times 10^5 \text{ M}^{-1} \text{ cm}^{-1}$ as molar absorbance⁵¹. Ultrapure water purified with a Direct-Q 3 UV apparatus (Millipore, USA) was used for the preparation of all aqueous solutions and suspensions.

Preparation of GUV suspensions. Most of the investigations presented were carried out with GUVs with a size range of 1–200 μm or even larger. They allow a direct quantitative analysis of changes in size and shape of individual vesicles by optical microscopy. GUVs composed of AOT were prepared by using the gentle hydration method⁵². First, AOT (17.8 mg) was dissolved in 1 mL chloroform in a glass vial. Then, a thin AOT film was prepared on the inner surface of the vial by using a nitrogen gas stream under rotation of the vial by hand. To remove the organic solvent completely, the AOT film was put under vacuum overnight, while the vial was kept wrapped with aluminium foil. The pre-warmed, dried AOT film was hydrated with 2.0 mL of a NaH_2PO_4 solution (20 mM, pH = 4.3) at 60°C for 1 h, which resulted in the formation of GUVs with radii of 5–30 μm . The obtained 20 mM AOT GUV suspension was stored at 25°C .

GUVs composed of phospholipids (DOPC, DOPA, DOPG, or DOPS) or sulfatide were prepared by using the same protocol. The final lipid concentrations in these suspensions were 5 mM. Binary GUVs composed of either AOT and cholesterol (9:1 or 95:5, molar ratio, 5 mM in total), or SDBS and DA (1:1 molar ratio, 20 mM in total) were prepared in the same way as described above from the corresponding chloroform solutions containing the appropriate mixture of the two amphiphiles. Please note that stable AOT/cholesterol GUVs could not be prepared for cholesterol contents above 10 mol%.

Preparation of LUV suspensions. To characterise the PANI products which were obtained in the presence of vesicles by UV/vis/NIR absorption spectroscopy, 20 mM AOT, 20 mM SDBS/DA (1:1), 5 mM phospholipids (DOPC, DOPA, DOPG, and DOPS) or 5 mM sulfatides, LUVs with a size range of ~100–1000 nm were prepared by using the freezing–thawing extrusion method in a similar way as described before²¹. First, GUV suspensions were prepared as described above. Then, the obtained GUV suspensions were frozen in liquid nitrogen and thawed in a water bath heated to 60 °C. This procedure was repeated ten times. After these freezing–thawing cycles, the phospholipid or sulfatide suspensions were extruded 21 times through a 100 nm pore size Nucleopore polycarbonate membrane, using a Mini Extruder set from Avanti Polar Lipids, Inc., USA. For the preparation of AOT and SDBS/DA (1:1) LUVs, the GUV suspensions were extruded ten times through a 200 nm pore size Nucleopore polycarbonate membrane, and then, ten times through a 100 nm pore size membrane, using a LIPEX™ Extruder from Northern Lipids Inc., Canada. The obtained LUVs were characterised previously by dynamic light scattering (DLS) and cryo transmission electron microscopy²¹. The LUVs had an average hydrodynamic diameter of about 80 nm with a polydispersity of about 0.1. The cvc value for AOT in 20 mM NaH_2PO_4 solution (pH = 4.3) was determined by turbidity measurements (1.5 mM), as described before for AOT in 100 mM NaH_2PO_4 solution (pH = 4.3) (0.4 mM)²².

Preparation of SUV suspensions and micellar solutions. SUV (sonicated, small unilamellar vesicles with a size range of ~20–100 nm) suspensions for the micro-injection experiments were obtained by sonication of the prepared GUV suspensions (see above) for 5 min at room temperature using a Branson Sonifier model 150 (Emerson, USA). AOT and SDBS micellar solutions were also prepared for the use in the micro-injection experiments by simply dissolving the two amphiphiles in deionized water. The SUV suspensions and the micellar solutions were mixed with an aqueous hydrogen peroxide solution just before use and then pressed through a 0.2 μm polypropylene filter (Puradisc 25 PP, from GE Healthcare UK Ltd., England).

The prepared AOT SUV suspension and the micellar solution were characterised by DLS. The obtained intermediate scattering function for 3.0 mM AOT SUV suspension was well described by a single exponential function. The cumulant analysis indicated that the AOT SUVs had an average hydrodynamic diameter of about 60 nm with a polydispersity of about 0.02. The scattering function for 20 mM AOT micelles in 2.0 M H_2O_2 solution was well described by two modes composed of a single exponential in shorter time region and a stretched exponential in longer time region, which is frequently observed for wormlike micelle solutions⁵³. The collective diffusion coefficient obtained from the single exponent mode was $5.2 \times 10^{-10} \text{ m}^2/\text{s}$ and the effective slow relaxation time from the stretched exponential mode is $2.1 \times 10^{-3} \text{ s}$.

Enzymatic polymerisation of aniline in the presence of LUVs. The enzymatic polymerisation of aniline in the presence of AOT LUVs or SDBS/DA (1:1) LUVs as templates was carried out in a 20 mM NaH_2PO_4 solution (pH = 4.3) at 25 °C following a protocol described before²³. All components of the reaction mixture, except H_2O_2 , were first added to 699.8 μL NaH_2PO_4 solution (20 mM, pH = 4.3): 150 μL LUV suspension (20 mM amphiphile in 20 mM NaH_2PO_4 solution), 100 μL aniline solution (40 mM in 20 mM NaH_2PO_4 solution, pH adjusted to 4.3 with H_3PO_4), and 47.9 μL HRP solution (2.2 mg HRP powder dissolved in 2.0 mL 20 mM NaH_2PO_4 solution, pH 4.3, yielding 19.2 μM HRP, spectrophotometrically determined). After mixing, the reaction was triggered by quick addition of 2.25 μL freshly prepared H_2O_2 solution (2.0 M in water). The initial concentrations in the reaction mixture were: 3.0 mM AOT, 4.0 mM aniline, 0.92 μM HRP and 4.5 mM H_2O_2 , pH = 4.3 (20 mM NaH_2PO_4). The reactions were carried out in Eppendorf safe-lock tubes, and the total reaction time was 24 h at room temperature. For the polymerisation using 5 mM LUV suspension (DOPC, DOPA, DOPG, and DOPS, and sulfatide), 600 μL of the LUV suspension and 249.8 μL NaH_2PO_4 solution (pH = 4.3) were mixed instead.

The products of the polymerisation reaction were examined by UV/vis/NIR absorption spectroscopy. For the reactions carried out without vesicles, the NaH_2PO_4 solution (pH = 4.3) was used instead of the LUV suspension.

Enzymatic polymerisation of aniline on GUVs. Changes in the size and morphology of GUVs in response to the enzymatic polymerisation of aniline coupled with feeding of the amphiphiles were analysed by phase contrast light microscopy (see below). The experiments were performed in the microscope sample chamber, which is a hole in a silicone rubber sheet placed onto a glass slide. The hole had a diameter of 12 mm and a depth of 1 mm. The GUV suspension mixed with the

polymerisation components, except H_2O_2 , was carefully transferred at room temperature from the glass vial into the sample chamber. The initial concentrations of the different components of the reaction mixture were the same as the ones for the polymerisation experiments with LUVs: 20 mM NaH_2PO_4 solution (pH = 4.3) containing 4.0 mM aniline and 0.92 μM HRP. The polymerisation was triggered by micro-injecting a 2.0 M H_2O_2 solution containing either SUVs (20 mM DOPC, DOPA or AOT), or micelles (20 mM AOT or 100 mM SDBS). The micro-pipette used for the micro-injection was a Femtotip II with an inner diameter of $0.5 \pm 0.2 \mu\text{m}$ (Eppendorf, Germany). The position of the micro-pipette was controlled using a hydraulic micro-manipulator MMO-202ND (Narishige, Japan), and the micro-injection was performed using a Femtojet system (Eppendorf, Germany). To minimize GUV drifts caused by the injection flow, we adopted a double micro-pipette injection technique with a symmetric configuration, where the target GUV was located at the bottom of the chamber (Supplementary Fig. 4). The two injection flows trap the GUV at a fixed point, which makes it possible to measure the growth of the GUV quantitatively with high reproducibility. The distance from the tip of the pipettes to the target GUV was about 100 μm and most of the micro-injection experiments were performed with an injection pressure of 180 hPa. The volume injected from the pipette was 0.14 nL/s. In additional experiments, single micro-injections were also performed, and the growth of the vesicles coupled to the aniline polymerisation was analysed.

Microscope observation of GUVs. The GUV growth in response to the micro-injection was followed by using an Axio Vert. A1 FL-LED inverted fluorescence microscope in phase contrast mode (Carl Zeiss, Germany) with a 40 \times objective (LD A-Plan 40 \times N.A. = 0.55) and an Axiocam 506mono (Carl Zeiss, Germany) for recording the images. To estimate the vesicle surface area (A) and volume (V), a 3D image of the GUV was reconstructed from the 2D microscope image by using the Surface Evolver software package^{6,35}.

UV/vis/NIR absorption measurements. Absorption measurements in the UV/vis/NIR region of the spectrum were recorded with a V-730 spectrometer (JASCO, Japan) at 25 °C, using quartz cuvettes S15-UV-1 (from GL Sciences Inc. Japan) with path lengths of 1 mm.

DLS measurements. Dynamic light scattering measurements were performed using an ALV-5000 goniometer system (ALV, Langen, Germany) with an ALV-6000 multi-bit multi-tau correlator and a diode-pumped laser Verdi V-2 (Coherent Inc. Santa Clara, USA) operating with vertically polarised light at $\lambda = 532 \text{ nm}$. The sample was filtered before the measurement with a 0.22 μm membrane filter (from Millipore).

Data availability

All the data generated or analysed during this study are included in this published article (and in the Supplementary Information). Further details are available from the corresponding author upon request.

Received: 22 February 2019; Accepted: 18 September 2019;

Published online: 11 October 2019

References

1. Szostak, J. W., Bartel, D. P. & Luisi, P. L. Synthesizing life. *Nature* **409**, 387–390 (2001).
2. Deamer, D. W. & Szostak, J. W. *The Origins of Life: A Subject Collection from Cold Spring Harbor Perspectives in Biology*. (Cold Spring Harbor Laboratory Press, 2010).
3. Luisi, P. L. & Stano, P. *The Minimal Cell: The Biophysics of Cell Compartment and the Origin of Cell Functionality*. (Springer Science & Business Media, 2010).
4. Rasmussen, S. et al. *Protocells – Bridging Nonliving and Living Matter*. (The MIT Press, Cambridge, 2008).
5. Sakuma, Y. & Imai, M. Model system of self-reproducing vesicles. *Phys. Rev. Lett.* **107**, 1–5 (2011).
6. Jimbo, T., Sakuma, Y., Urakami, N., Zihler, P. & Imai, M. Role of inverse-cone-shape lipids in temperature-controlled self-reproduction of binary vesicles. *Biophys. J.* **110**, 1551–1562 (2016).
7. Urakami, N., Jimbo, T., Sakuma, Y. & Imai, M. Molecular mechanism of vesicle division induced by coupling between lipid geometry and membrane curvatures. *Soft Matter* **14**, 3018–3027 (2018).
8. Imai, M. & Walde, P. In *The Giant Vesicle Book* (eds Dimova, R. & Marques, C.) (CRC Press, 2019).
9. Morigaki, K., Walde, P., Misran, M. & Robinson, B. H. Thermodynamic and kinetic stability. Properties of micelles and vesicles formed by the decanoic acid/decanoate system. *Colloids Surf. A Physicochem. Eng. Asp.* **213**, 37–44 (2003).

10. Walde, P., Wick, R., Fresta, M., Mangone, A. & Luisi, P. L. Autopoietic self-reproduction of fatty acid vesicles. *J. Am. Chem. Soc.* **116**, 11649–11654 (1994).
11. Wick, R., Walde, P. & Luisi, P. L. Light microscopic investigations of the autocatalytic self-reproduction of giant vesicles. *J. Am. Chem. Soc.* **117**, 1435–1436 (1995).
12. Zepik, H. H., Walde, P. & Ishikawa, T. Vesicle formation from reactive surfactants. *Angew. Chem. - Int. Ed.* **47**, 1323–1325 (2008).
13. Zhu, T. F. & Szostak, J. W. Coupled growth and division of model protocell membranes. *J. Am. Chem. Soc.* **131**, 5705–5713 (2009).
14. Budin, I., Debnath, A. & Szostak, J. W. Concentration-driven growth of model protocell membranes. *J. Am. Chem. Soc.* **134**, 20812–20819 (2012).
15. Adamala, K. & Szostak, J. W. Competition between model protocells driven by an encapsulated catalyst. *Nat. Chem.* **5**, 495–501 (2013).
16. Takakura, K. & Sugawara, T. Membrane dynamics of a myelin-like giant multilamellar vesicle applicable to a self-reproducing system. *Langmuir* **20**, 3832–3834 (2004).
17. Takakura, K., Toyota, T. & Sugawara, T. A novel system of self-reproducing giant vesicles. *J. Am. Chem. Soc.* **125**, 8134–8140 (2003).
18. Kurihara, K. et al. Self-reproduction of supramolecular giant vesicles combined with the amplification of encapsulated DNA. *Nat. Chem.* **3**, 775–781 (2011).
19. Hardy, M. D. et al. Self-reproducing catalyst drives repeated phospholipid synthesis and membrane growth. *Proc. Natl Acad. Sci. USA* **112**, 8187–8192 (2015).
20. Seoane, A., Brea, R. J., Fuertes, A., Podolsky, K. A. & Devaraj, N. K. Biomimetic Generation and Remodeling of Phospholipid Membranes by Dynamic Imine Chemistry. *J. Am. Chem. Soc.* **140**, 8388–8391 (2018).
21. Junker, K. et al. Mechanistic aspects of the horseradish peroxidase-catalysed polymerisation of aniline in the presence of AOT vesicles as templates. *RSC Adv.* **2**, 6478–6495 (2012).
22. Guo, Z., Hauser, N., Moreno, A., Ishikawa, T. & Walde, P. AOT vesicles as templates for the horseradish peroxidase-triggered polymerization of aniline. *Soft Matter* **7**, 180–193 (2011).
23. Guo, Z. et al. Vesicles as soft templates for the enzymatic polymerization of aniline. *Langmuir* **25**, 11390–11405 (2009).
24. Foreman, J. P. & Monkman, A. P. Theoretical investigations into the structural and electronic influences on the hydrogen bonding in doped polyaniline. *Synth. Met.* **107**, 7604–7610 (2003).
25. Luginbühl, S. et al. The influence of anionic vesicles on the oligomerization of *p*-aminodiphenylamine catalyzed by horseradish peroxidase and hydrogen peroxide. *Synth. Met.* **226**, 89–103 (2017).
26. Luginbühl, S., Bertschi, L., Willeke, M., Schuler, L. D. & Walde, P. How Anionic Vesicles Steer the Oligomerization of Enzymatically Oxidized *p*-Aminodiphenylamine (PADPA) toward a Polyaniline Emeraldine Salt (PANI-ES)-Type Product. *Langmuir* **32**, 9765–9779 (2016).
27. Kauffman, S. A. Autocatalytic sets of proteins. *J. Theor. Biol.* **119**, 1–24 (1986).
28. Kaneko, K. & Yomo, T. On a kinetic origin of heredity: minority control in a replicating system with mutually catalytic molecules. *J. Theor. Biol.* **214**, 563–576 (2002).
29. Hait, S. K., Majhi, P. R., Blume, A. & Moulik, S. P. A Critical Assessment of Micellization of Sodium Dodecyl Benzene Sulfonate (SDBS) and Its Interaction with Poly(vinyl pyrrolidone) and Hydrophobically Modified Polymers, JR 400 and LM 200. *J. Phys. Chem. B* **107**, 3650–3658 (2003).
30. Namani, T. & Walde, P. From decanoate micelles to decanoic acid/dodecylbenzenesulfonate vesicles. *Langmuir* **21**, 6210–6219 (2005).
31. Liu, W., Kumar, J., Tripathy, S., Senecal, K. J. & Samuelson, L. Enzymatically synthesized conducting polyaniline. *J. Am. Chem. Soc.* **121**, 71–78 (1999).
32. do Nascimento, G. M. & de Souza, M. A. In *Nanostructured Conductive Polymers*. (ed. Eftekhari, A.) (John Wiley & Sons, Chichester, 2015).
33. Huang, W. S. & MacDiarmid, A. G. Optical properties of polyaniline. *Polymer* **34**, 1833–1845 (1993).
34. Nave, S., Eastoe, J. & Penfold, J. What is so special about aerosol-OT? 1. Aqueous systems. *Langmuir* **16**, 8733–8740 (2000).
35. Brakke, K. A. The surface evolver. *Exp. Math.* **1**, 141–165 (1992).
36. Liu, W. et al. The role of template in the enzymatic synthesis of conducting polyaniline. *J. Am. Chem. Soc.* **121**, 11345–11355 (1999).
37. Berclaz, N., Müller, M., Walde, P. & Luisi, P. L. Growth and transformation of vesicles studied by ferritin labeling and cryotransmission electron microscopy. *J. Phys. Chem. B* **105**, 1056–1064 (2001).
38. Seifert, U. Configurations of fluid membranes and vesicles. *Adv. Phys.* **46**, 13–137 (1997).
39. Sakashita, A., Urakami, N., Zihler, P. & Imai, M. Three-dimensional analysis of lipid vesicle transformations. *Soft Matter* **8**, 8569–85818 (2012).
40. Seifert, U., Berndt, K. & Lipowsky, R. Shape transformations of vesicles: Phase diagram for spontaneous curvature and bilayer-coupling models. *Phys. Rev. A* **44**, 1182–1202 (1991).
41. Fourcade, B., Miao, L., Pao, M. & Wortis, M. Scaling analysis of narrow necks in curvature models of fluid-bilayer vesicles. *Phys. Rev. E* **49**, 5276–5287 (1994).
42. Döbereiner, H. G., Käs, J., Noppl, D., Sprenger, I. & Sackmann, E. Budding and fission of vesicles. *Biophys. J.* **65**, 1396–1403 (1993).
43. Chen, C. M., Higgs, P. G. & Mac Kintosh, F. C. Theory of fission for two-component lipid vesicles. *Phys. Rev. Lett.* **79**, 1579–1582 (1997).
44. Lindblom, G. & Wennerström, H. Amphiphile diffusion in model membrane systems studied by pulsed NMR. *Biophys. Chem.* **6**, 167–171 (1977).
45. Gánti, T. Biogenesis itself. *J. Theor. Biol.* **187**, 583–593 (1997).
46. Mansy, S. S. In *The Origin of Life* (eds Deamer, D. & Szostak, J. W.) 193–206 (Cold Spring Harbor Laboratory Press, New York, 2010).
47. Monnard, P. A. & Deamer, D. W. In *The Minimal cell: the biophysics of cell compartment and the origin of cell functionality*. (eds Luisi, P. L. & Stano, P.) 123–151 (Springer Science & Business Media, 2010).
48. Rasmussen, S., Constantinescu, A. & Svaneborg, C. Generating minimal living systems from non-living materials and increasing their evolutionary abilities. *Philos. Trans. R. Soc. B Biol. Sci.* **371**, 20150440 (2016).
49. Serra, R., Carletti, T. & Poli, I. Synchronization phenomena in surface-reaction models of protocells. *Artif. Life* **13**, 123–138 (2007).
50. Von Neumann, J. *Theory of Self-reproducing Automata*. (University of Illinois Press, 1966).
51. Dunford, H. B. & Stillman, J. S. On the function and mechanism of action of peroxidases. *Coord. Chem. Rev.* **19**, 187–251 (1976).
52. Reeves, J. P. & Dowben, R. M. Formation and properties of thin-walled phospholipid vesicles. *J. Cell. Physiol.* **73**, 49–60 (1969).
53. Moitzi, C., Freiburger, N. & Glatzer, O. Viscoelastic wormlike micellar solutions made from nonionic surfactants: structural investigations by SANS and DLS. *J. Phys. Chem. B* **109**, 16161–16168 (2005).

Acknowledgements

This work was in part supported by JSPS KAKENHI Grant Numbers JP25247070, JP16H02216, JP17K14368 and JSPS KAKENHI “Fluctuation and Structure” Grant Number JP25103009. We thank Prof. Toshihiro Kawakatsu (Tohoku University) for helpful discussions.

Author contributions

M.K., M.I. and P.W. conceived the work, designed the experiments and wrote the manuscript with input from all other authors. M.K. conducted experiments. H.A., S.S.-L. and P.W. established the “template” polymerisation of aniline on AOT GUVs. T.J. and Y.S. developed the vesicle division induced by adding second amphiphile and analysed the reproduction pathway.

Competing interests

The authors declare no competing interests.

Additional information

Supplementary information is available for this paper at <https://doi.org/10.1038/s42004-019-0218-0>.

Correspondence and requests for materials should be addressed to M.I.

Reprints and permission information is available at <http://www.nature.com/reprints>

Publisher's note Springer Nature remains neutral with regard to jurisdictional claims in published maps and institutional affiliations.



Open Access This article is licensed under a Creative Commons Attribution 4.0 International License, which permits use, sharing, adaptation, distribution and reproduction in any medium or format, as long as you give appropriate credit to the original author(s) and the source, provide a link to the Creative Commons license, and indicate if changes were made. The images or other third party material in this article are included in the article's Creative Commons license, unless indicated otherwise in a credit line to the material. If material is not included in the article's Creative Commons license and your intended use is not permitted by statutory regulation or exceeds the permitted use, you will need to obtain permission directly from the copyright holder. To view a copy of this license, visit <http://creativecommons.org/licenses/by/4.0/>.

© The Author(s) 2019